Electrostatic and dynamical effects of an aqueous solution on the zero-bias conductance of a single molecule: A first-principles study

Arihiro Tawara,* Tomofumi Tada, and Satoshi Watanabe
Department of Materials Engineering, The University of Tokyo, 7-3-1 Hongo, Bunkyo-ku, Tokyo 113-8656, Japan
and CREST, Japan Science and Technology Agency, 5 Sanbancho, Chiyoda-ku, Tokyo 102-0075, Japan
(Received 7 July 2009; published 26 August 2009)

The electrostatic and dynamical effects of an aqueous solution on the conductance of benzene-1,4-dithiolate are examined using the *ab initio* nonequilibrium Green's function method and Car-Parrinello molecular dynamics. The peak of the conductance histogram shifts downward by 0.01–0.02 G_0, which is attributed to the electrostatic effects of the aqueous solution. Dynamical changes in molecular motion induced by the aqueous solution are observed in the molecular dynamics, resulting in emergence/disappearance of new peaks in the conductance histograms.

DOI: 10.1103/PhysRevB.80.073409 PACS number(s): 31.15.A−, 85.65.+h, 73.63.−b

In recent years, electronic-transport properties of single molecular junctions have been investigated in experimental and theoretical studies to explore possible applications such as nanostructured devices. Benzene-1,4-dithiolate (BDT) between gold electrodes has been used as a benchmark molecule in such experimental[1–4] and *ab initio* theoretical studies.[5–8] In experimental studies, the observed values of conductance of the BDT molecule ranges from 10^{-4} to 10^{-2} $G_0(=2e^2/h)$.[1–4] On the other hand, the BDT conductance calculated using the density-functional theory (DFT) (Ref. 9) and nonequilibrium Green's function (NEGF) method[10] are about 0.4 G_0.[7,8] The difference in conductance between experimental and theoretical studies is a well-known problem of single molecular conductance. In a quantitative comparison, however, we must take into account the experimental/theoretical conditions used in these studies: most of the observed conductances were obtained at room temperature and in solution,[1–3] whereas the calculated conductances were obtained assuming 0 K and a vacuum environment.[5–8] Several experimental works were devoted to addressing the temperature and solution effects on the electronic conductance of a single molecule. Li and co-workers observed no solution or temperature effects on conductance[11] while Grüter *et al.* observed solution effects especially in the low-conductance ($\ll G_0$) regime.[12] In theoretical studies, various effects such as adsorption configuration,[13–17] inelastic current,[18–22] and limitation of DFT (Refs. 23–26) have been studied extensively, which contributed to our understanding of the transport properties of molecular junctions. However, solution effects on conductance of single molecules have not been explored in theoretical fashion so far.

Since the observed conductance fluctuates considerably and is usually analyzed through histograms, theoretical analyses based on conductance histograms are expected to provide a better understanding of the electronic transport through a single molecule. Andrews *et al.* calculated BDT conductances in a vacuum for a large number of BDT configurations by the NEGF method and obtained conductance histograms.[27] However, their method based on the extended Hückel method is not reliable enough. This approach has not yet been reported on the DFT level, except for a DFT study assuming random fluctuations of configurations.[28]

In this Brief Report, we report our calculation of a large number of conductances of a BDT molecule sandwiched between Au(100) surfaces, in which BDT is surrounded by an aqueous solution of 1.0 g/cm^3, using the *ab initio* NEGF-DFT method and Car-Parrinello molecular dynamics (CPMD). We used the Au(100) contact as electrodes in stead of more realistic Au(111) one intentionally because our objective is to extract bare effects of aqueous solution on conductance and adsorption structures of thiolate molecules on Au(111) are complex.[29]

Analysis of the results including conductance histograms clearly reveals the effects of the aqueous solution surrounding the BDT. For comparison, we also investigate the molecular junction without the aqueous solution. We abbreviate the systems with and without the aqueous solution as Au(100)/BDT+water/Au(100) and Au(100)/BDT/Au(100), respectively.

We adopted the following computational procedures: we first perform CPMD calculations using the code[30,31] (Step I) and then NEGF-DFT calculations using the code ATOMISTIX TOOLKIT (ATK) (Refs. 32–35) (Step II) to obtain zero-bias conductances for configurations selected from the results of Step I. Finally, we make histograms of the calculated conductances (STEP III).

To begin with, we obtain the initial structure of Au(100)/BDT/Au(100) using ATK calculation with Perdew, Burke, and Ernzerhof (PBE) functional[36] of the generalized gradient approximation (GGA) and single zeta polarization numerical atomic orbitals. Number of k points is 4×4, which is confirmed to be enough in this system. Electron temperature is set to 300 K. The hollow-site adsorption with an interelectrode distance of 9.8 Å is assumed which was found to be the most stable among adsorption sites on the Au(100) surface.

The initial configuration of water molecules in Au(100)/BDT+water/Au(100) was determined using the MM2 force-field calculation[37] and subsequent annealing in CPMD. In the annealing processes, the BDT molecule adsorbed at the hollow site is fixed to the structure optimized by the ATK calculation.

In the CPMD calculations (Step I), we performed three types of molecular dynamics: in MD1, the BDT molecule is

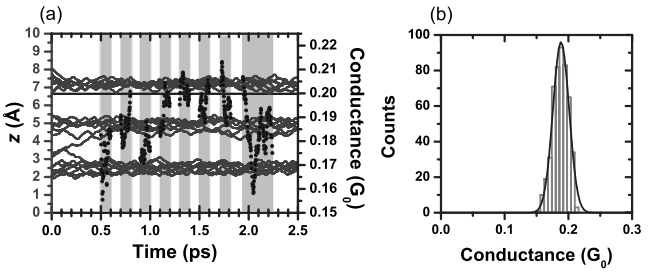

FIG. 1. (a) Calculated time evolution of oxygen positions (thin lines) and conductance (points) of BDT in the aqueous solution. Here, the z axis is perpendicular to the Au(100) surface and $z=0$ and 9.8 Å correspond to the topmost layers of the Au(100) surfaces. The thick line shows the conductance value of BDT without water. (b) Calculated conductance histogram using CONF1 of Au(100)/BDT+water/Au(100).

fixed to the above optimized position (i.e., only water molecules are relaxed). Water and BDT molecules are relaxed in MD2, and the BDT molecule without water is relaxed in MD3. We abbreviate the configurations obtained in MD1, MD2, and MD3 as CONF1, CONF2, and CONF3, respectively. Note that Au atoms are fixed during the dynamics in all simulations. The unit cell in the CPMD calculations includes 22 H_2O (1.0 g/cm^3), BDT attached to the Au(100) surfaces, and seven gold layers composed of nine (3×3) gold atoms per layer. The CPMD calculations were performed using the PBE functional[36] of GGA and Vanderbilt ultrasoft pseudopotentials[38] with a cut-off energy of 35 Ry. We adopted a fictitious electron mass of 1100 a.u. and a time step of 4 a.u. (0.097 fs) at 300 K. The temperature is controlled with the Nose-Hoover thermostat.[39,40] In the conductance calculations (Step II), the scattering region is composed of a BDT, 22 H_2O, and three gold layers constituted by nine gold atoms per layer for each electrode.

Figure 1(a) shows the time evolution for 2.5 ps of the z positions of oxygen atoms in MD1 and the zero-bias conductances of Au(100)/BDT+water/Au(100) using CONF1. We found that water molecules trapped between the electrodes form a layer structure with an interlayer distance of about 2.5 Å. Three layers of water are clearly visible after 0.5 ps (equilibration) of the CPMD simulation and the numbers of water molecules in each layer is 7, 7, and 8 (abbreviated as Water778 hereafter) from the upper to lower layers in Fig. 1(a). The uppermost and lowermost layers of water appear at about 2.5 Å apart from the gold surface showing good agreement with other simulations of water/metal interfaces.[41]

We picked up a single configuration per 20 steps (1.94 fs) in the CPMD simulation in the shaded regions in Fig. 1(a) and calculated the zero-bias conductances for the selected configurations using ATK. We note that the physical meaning of the time evolution of the calculated conductance is unclear because the configurations used in the conductance calculations are not obtained by ATK but CPMD. However, the configurations obtained in CPMD are expected to form a good set for statistical evaluations of conductances using ATK. Thus, we focused on using the conductance histogram.

Figure 1(b) shows the conductance histogram using a bin size of 0.006 G_0 constructed from ~500 selected configurations. Fitting the histogram with a Gaussian, we estimated the peak position to be 0.188 G_0 and the standard deviation to be ±0.013 G_0. The peak position is 6.5% smaller than the conductance value for Au(100)/BDT/Au(100), 0.201 G_0. Here, the number of samples and bin size in the histogram are checked carefully to fit it reasonably with the Gaussian. Since the BDT molecule is fixed in MD1, the peak shift and standard deviation clearly result from the interactions between the water molecules and BDT. To elucidate the effect of water molecules on conductance, we analyzed the effective potentials and electron densities for several configurations corresponding to the conductance values of 0.175 G_0, 0.185 G_0, and 0.200 G_0. Figures 2(a) and 2(b) show, respectively, the difference in effective potential and electron densities between the configuration with water having 0.175 G_0 and the configuration without water. The effective potential around the benzene ring is higher in the configuration with water than in that without water, which corresponds to the decrease in conductance in the presence of water molecules. The rise of effective potential around BDT is also confirmed in other configurations (0.175 G_0 and 0.185 G_0) but no such change in effective potential is seen in configurations of 0.200 G_0. Figure 2(b) shows the charge transfer from water molecules to BDT. In contrast to the effective potential, the charge transfer from water molecules to BDT of about $0.1e^-$ in Mulliken charge is seen in all configurations. Thus, we conclude that the conductance decrease induced by water molecules is not due to the charge transfer between the water and BDT but to the electrostatic effect from the dipole moments of water molecules.

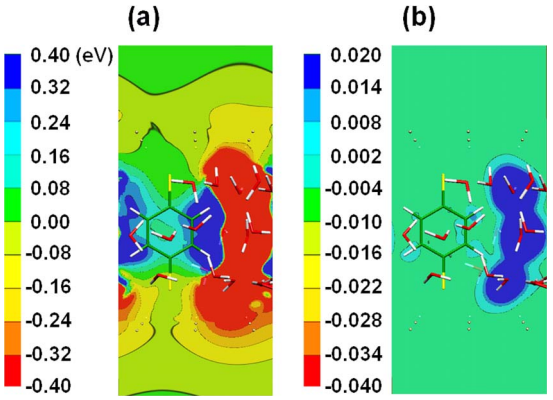

FIG. 2. (Color online) The differences in (a) effective potential and (b) electron density between the configuration with water having a conductance of 0.175 G_0 and the configuration without water. Effective potential and electron-density differences are depicted on the benzene plane.

We also considered other water structures having 8, 6, and 8 (Water868) and 7, 6, and 9 (Water769) molecules in respective layers. Note that the two- and four-layer structures are energetically unstable for water molecules of 1.0 g/cm^3 in a nanogap of 9.8 Å. The peak positions and standard deviations, which are evaluated by fitting the histograms with a Gaussian, are almost the same for Water868 and Water778, while the peak position in the Water769 case, 0.178 G_0, is clearly different from the others and 11.4% smaller than the conductance of the configuration without water. Thus, we

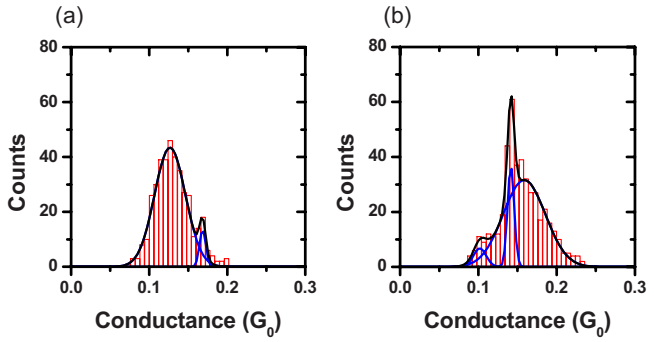

FIG. 3. (Color online) Calculated conductance histograms using (a) CONF2 (Water769) of Au(100)/BDT+water/Au(100) and (b) CONF3 of Au(100)/BDT/Au(100). The curves denote the respective Gaussian functions obtained by the fitting and the sum of the Gaussians.

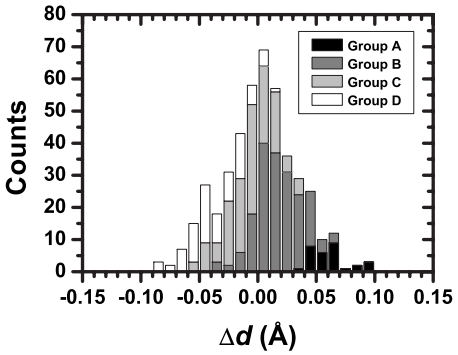

FIG. 4. C-S bond-length histogram in MD3 (without water). The total histogram is divided into four groups depending on the conductance value G: (Group A) $G<0.110\ G_0$, (Group B) $0.110\ G_0 \leq G<0.150\ G_0$, (Group C) $0.150\ G_0 \leq G<0.180\ G_0$, and (Group D) $0.180\ G_0<G$.

can say that the difference in the local concentration of water affects the transport properties of the single BDT. It is worth mentioning that the average total energy in the Water769 configuration is higher than that in Water778 and Water868 by 2.16 and 1.49 eV per unit cell, respectively. However, such unstable configurations easily appear in BDT-relaxed simulations (MD2), as described later.

To obtain further insight into the dynamical effects of water molecules on BDT conductance, we performed MD2/MD3-type simulations, in which BDT and water molecules are relaxed. The same initial configuration as in MD1 was used. The CPMD simulation at 300 K was performed for 1.6 ps including equilibration. The Water769 layer structure appeared in MD2 after 0.5 ps.

Figures 3(a) and 3(b) show the conductance histogram obtained using CONF2 and CONF3, respectively. The bin size of both the histograms is $0.006\ G_0$. By comparing Figs. 1(b) and 3, we can clearly see that the fluctuation in conductance is larger in the CONF2 and CONF3 histograms (Fig. 3) than in the CONF1 histogram [Fig. 1(b)]. This difference can be attributed to the structural fluctuations of the BDT molecule. In addition, the positions of the main peaks ($0.125\ G_0$ in the CONF2 histogram and $0.159\ G_0$ in the CONF3 histogram) are significantly different from the peak in the CONF1 histogram and conductance value without water. These large differences in the peak position are an artifact of our computational procedure: the structure of BDT optimized with the ATK code was used in MD1, whereas the BDT structure fluctuates around the stable position derived from the effective potentials by CPMD calculations in MD2 and MD3. Since the conductance value of BDT (without water) using the structure optimized with CPMD (Ref. 42) is calculated to be $0.147\ G_0$, we can say that the electrostatic influence of the aqueous solution shifts the peak from $0.147\ G_0$ (without water) to $0.125\ G_0$ (Water769) in the CONF2 histogram. The peak shift of $-0.022\ G_0$ corresponds well to the electrostatic effect due to the aqueous solution found in Water769 in MD1.

Another important feature found in CONF2/3 histograms is the emergence of several new peaks in the conductance histograms. Fitting the histograms with several Gaussian functions, we found two peaks in the CONF2 histogram (Water769) and three in the CONF3 histogram (without water). The peak positions/standard deviations of the respective Gaussians are $0.127\ G_0/\pm 0.020\ G_0$ and $0.168\ G_0/\pm 0.004\ G_0$ in the CONF2 histogram, and $0.159\ G_0/\pm 0.027\ G_0$, $0.142\ G_0/\pm 0.005\ G_0$, and $0.102\ G_0/\pm 0.008\ G_0$ in the CONF3 histogram. The peak at $0.102\ G_0$ obtained in the CONF3 histogram disappears in the CONF2 histogram while the peak at $0.168\ G_0$ in the CONF2 histogram is not confirmed in the CONF3 histogram. To understand the cause of the peak emergence/disappearance, we analyze the dynamics of BDT in MD2 and MD3 by focusing on the peak at $0.102\ G_0$. We found that the dynamical fluctuations of the adsorption sites of BDT on Au(100) are quite small in both MD2 and MD3 while those of the C-S bond length differ between the two MD simulations. To determine the correlation between the C-S bond length and conductance, we divide the CONF3 histogram into four groups in terms of the conductance G: (Group A) $G<0.110\ G_0$, (Group B) $0.110\ G_0 \leq G<0.150\ G_0$, (Group C) $0.150\ G_0 \leq G<0.180\ G_0$, and (Group D) $0.180\ G_0<G$. Figure 4 shows the C-S bond-length histogram with showing a breakdown by this grouping. Note that the BDT molecule has two C-S bonds and their average was used in the bond-length histogram. In the histogram, Δd corresponds to the difference of the bond length from the optimized value ($d_{\mathrm{opt}}=1.81$ Å). Group A is almost perfectly constituted of the BDT configurations with a C-S bond length of 1.91 -1.85 Å. Thus, the conductance peak at $0.102\ G_0$ can be assigned to the BDT configurations with lengthened C-S bonds. On the other hand, no such conductance peak is obtained at $0.102\ G_0$ in the CONF2 histogram (Water769) and the number of BDT configurations with lengthened C-S bonds in MD2 (Water769) is less than that in MD3 (without water), which indicates that the water molecules clearly affect the dynamics, especially the C-S stretching mode of the BDT molecular junction. We also analyzed the origin of the peak at $0.168\ G_0$ in the CONF2 histogram and confirmed that the large conductances ($>0.168\ G_0$) result from the configurations with shortened C-S bond structures (not shown). It is worth mentioning that the correlation between the Au-S bond length and conductance is hardly seen in our

system in contrast to Ref. 17. This discrepancy may be due to the difference in computational condition: The BDT geometry is fixed while the Au electrode distance changes with the Au-S bond length in Ref. 17. Thus, we can say that the motion of the BDT junction is dynamically affected by the surrounding water molecules, leading to the peak emergence/disappearance in conductance histograms.

In summary, we have examined the effects of an aqueous solution on the conductance of benzene-1,4-dithiolate at room temperature using the *ab initio* nonequilibrium Green's function method and Car-Parrinello molecular dynamics. We showed that the peak shifts in the conductance histogram of $0.01-0.02$ G_0 occurs by electrostatic effects of the aqueous solution. We also found that the conductance peaks can be decomposed into a few peaks. Furthermore, subsidiary peaks emerge or disappear due to dynamical effects of the aqueous solution, which is correlated with the change in the C-S stretching mode of the BDT molecular junction.

The present work was partially supported by the Grant-in-Aid for Scientific Research on Priority Area "Linked molecule in nanoscale (448)" and for Global COE Program "Global Center of Excellence for Mechanical Systems Innovation" by the Ministry of Education, Culture, Sports, Science and Technology of Japan. The authors thank S. Kasamatsu for his valuable comments. A part of the calculations was carried out on the SR11000 supercomputer at the Institute for Solid State Physics, The University of Tokyo.

*tawara@cello.t.u-tokyo.ac.jp

[1] M. A. Reed *et al.*, Science **278**, 252 (1997).
[2] X. Xiao *et al.*, Nano Lett. **4**, 267 (2004).
[3] M. Kiguchi *et al.*, Appl. Phys. Lett. **89**, 213104 (2006).
[4] E. Lörtscher, H. B. Weber, and H. Riel, Phys. Rev. Lett. **98**, 176807 (2007).
[5] S. N. Yaliraki *et al.*, J. Chem. Phys. **111**, 6997 (1999).
[6] M. Di Ventra, S. T. Pantelides, and N. D. Lang, Phys. Rev. Lett. **84**, 979 (2000).
[7] K. Stokbro *et al.*, Comput. Mater. Sci. **27**, 151 (2003).
[8] H. Kondo, H. Kino, J. Nara, T. Ozaki, and T. Ohno, Phys. Rev. B **73**, 235323 (2006).
[9] P. Hohenberg and W. Kohn, Phys. Rev. **136**, B864 (1964).
[10] S. Datta, *Electronic Transport in Mesoscopic Systems* (Cambridge University Press, Cambridge, 1995).
[11] X. Li *et al.*, J. Am. Chem. Soc. **128**, 2135 (2006).
[12] L. Grüter *et al.*, Small **1**, 1067 (2005).
[13] A. M. Bratkovsky and P. E. Kornilovitch, Phys. Rev. B **67**, 115307 (2003).
[14] S. Tanibayashi *et al.*, Jpn. J. Appl. Phys. **44**, 7729 (2005).
[15] R. B. Pontes *et al.*, J. Am. Chem. Soc. **128**, 8996 (2006).
[16] A. Grigoriev, J. Skoldberg, G. Wendin, and Z. Crljen, Phys. Rev. B **74**, 045401 (2006).
[17] D. Q. Andrews *et al.*, J. Chem. Phys. **125**, 174718 (2006).
[18] M. Galperin *et al.*, J. Chem. Phys. **121**, 11965 (2004).
[19] Y.-C. Chen *et al.*, Nano Lett. **4**, 1709 (2004).
[20] Y. Asai, Phys. Rev. Lett. **94**, 099901(E) (2005).
[21] T. Yamamoto, K. Watanabe, and S. Watanabe, Phys. Rev. Lett. **95**, 065501 (2005).
[22] N. Sergueev, D. Roubtsov, and H. Guo, Phys. Rev. Lett. **95**, 146803 (2005).
[23] P. Delaney and J. C. Greer, Phys. Rev. Lett. **93**, 036805 (2004).
[24] N. Sai, M. Zwolak, G. Vignale, and M. Di Ventra, Phys. Rev. Lett. **94**, 186810 (2005).
[25] B. Muralidharan, A. W. Ghosh, and S. Datta, Phys. Rev. B **73**, 155410 (2006).
[26] C. Toher and S. Sanvito, Phys. Rev. Lett. **99**, 056801 (2007).
[27] D. Q. Andrews *et al.*, Nano Lett. **8**, 1120 (2008).
[28] Y. Hu, Y. Zhu, H. Gao, and H. Guo, Phys. Rev. Lett. **95**, 156803 (2005).
[29] A. Cossaro *et al.*, Science **321**, 943 (2008).
[30] R. Car and M. Parrinello, Phys. Rev. Lett. **55**, 2471 (1985).
[31] CPMD, Copyright IBM Corp 1990–2006, Copyright MPI für Festkörperforschung Stuttgart 1997–2001.
[32] ATK manual and ATK version, 2.0, ATOMISTIX A/S www.quantumwise.com
[33] M. Brandbyge, J. L. Mozos, P. Ordejon, J. Taylor, and K. Stokbro, Phys. Rev. B **65**, 165401 (2002).
[34] J. M. Soler *et al.*, J. Phys.: Condens. Matter **14**, 2745 (2002).
[35] J. Taylor, H. Guo, and J. Wang, Phys. Rev. B **63**, 245407 (2001).
[36] J. P. Perdew, K. Burke, and M. Ernzerhof, Phys. Rev. Lett. **77**, 3865 (1996).
[37] U. Burkert and N. L. Allinger, *Molecular Mechanics* (American Chemical Society, Washington, DC, 1982).
[38] D. Vanderbilt, Phys. Rev. B **41**, 7892 (1990).
[39] S. Nose, J. Chem. Phys. **81**, 511 (1984).
[40] W. G. Hoover, Phys. Rev. A **31**, 1695 (1985).
[41] S. Izvekov and G. A. Voth, J. Chem. Phys. **115**, 7196 (2001).
[42] The difference in optimized structures of BDT is seen between ATK and CPMD, especially in the C-S bond lengths (1.75 and 1.81 Å with ATK and CPMD, respectively).